Investigation and Classification of Field Leakage Current Waveforms

Dionisios Pylarinos
High Voltage Lab, Department of Electrical and Computer Engineering,
University of Patras, 26504, Rio, Patras, Greece

Konstantinos Theofilatos
Pattern Recognition Lab, Department of Computer Engineering and Informatics,
University of Patras, 26504, Greece

Kiriakos Siderakis
Electrical Engineering Dept., School of Applied Technology,
Technological Educational Institute of Crete, P.O.Box 1939, GR. 71004, Iraklion, Greece

Emmanuel Thalassinakis
Public Power Corporation (P.P.C.),
Terma Kastorias Str, Katsambas, 71307, Iraklion, Greece

Isidoros Vitellas
Public Power Corporation (P.P.C.),
27 Patision Str, Athens, 10432, Greece

Antonio T. Alexandridis
Department of Electrical and Computer Engineering,
University Of Patras, 26504, Rio, Patras, Greece

and **Eleftheria Pyrgioti**
Department of Electrical and Computer Engineering,
University Of Patras, 26504, Rio, Patras, Greece

ABSTRACT

Leakage current (LC) monitoring is a widely employed tool for the investigation of surface electrical activity and the performance of high voltage insulators. Surface activity is correlated to the shape of LC waveforms. Although field monitoring is necessary in order to acquire an exact view of activity and insulators' performance, field waveforms are not often recorded due to the required long term monitoring and the accumulation of data. Instead, extracted values, such as the peak value, charge and number of pulses exceeding predefined thresholds, are recorded, with actual waveforms either being recorded occasionally or not at all. However, a fully representative extracted value is yet to be determined. In this paper, 1540 field waveforms are investigated to acquire a detailed image of the waveforms' shape in the field. Simple classification rules are employed to distinguish between basic groups. Discharge waveforms are further classified based on the duration of discharges. Twenty different features, from time and frequency domain, two feature extraction algorithms (student t-test and mRMR) and three classification algorithms (knn, Naïve Bayes, Support Vector Machines) are employed for the classification. Results described in this paper can be used to maximize the efficiency of field LC monitoring.

Index Terms - Leakage current, insulators, insulator contamination, feature extraction, feature selection, pattern classification.

1 INTRODUCTION

LEAKAGE Current (LC) monitoring is a widely applied technique for monitoring the electrical phenomena experienced on outdoor insulators and evaluate insulators' performance. On ceramic insulators activity mainly consists of dry band arcs that, under favorable conditions, may lead to flashover [1-3]. In case of non ceramic insulators, hydrophobic surface retains water in the form of droplets, but hydrophobicity loss periods are also experienced and therefore activity may consist of corona discharges as well as dry band arcs [4-5].

LC monitoring has been applied on various specimens, under a large variety of conditions [6]. The basics stages of activity have been correlated with certain waveform shapes. At the very first stage of activity, insulator acts as a capacitor and LC is sinusoid and capacitive [7-9]. As surface becomes conductive, a sinusoid resistive current is recorded, and as activity advances the waveform gets distorted [7, 9-12]. Advance from sinusoids to distorted sinusoids may be rapid and pure sinusoids may even not be recorded at all [13-14]. Distortion at this stage has been correlated to surface condition and the chemical content of the pollution layer [7, 15-19]. At the next stage, pulses are recorded on the waveform's crest [11-12, 20]. Smaller pulses have been correlated with point and filamentary discharges. As stronger discharges appear, pulses become larger and more frequent [9-13, 20-21]. It should be noted that isolated large pulses have also been recorded in some cases [10, 13, 22]. At the next stage, consequent large pulses are recorded, giving the waveform a symmetrical shape, [10-13]. This is considered to be the final stage prior to flashover.

It should be noted that, although surface activity is linked to the shape of LC waveforms, continuous waveform recording and investigation has been applied only in the laboratory, whereas in the field, waveforms are recorded intermittently or not at all [6], due to the long term monitoring required and the size of acquired data. Several techniques have been applied on LC waveforms in order to extract representative information [6]. In the case of field monitoring, the most commonly extracted values are the peak value, the charge and the number of pulses exceeding pre-defined thresholds, whereas the harmonic content is an added commonly investigated value in the case of laboratory measurements [6]. However, a fully representative value of the LC waveform's shape is yet to be determined. Classification and pattern recognition techniques have been also applied in order to cope with the problem, but only in case of laboratory measurements [6] or small sets of field measurements [23]. The complexity of field waveforms [24, 25] however, hints that further investigation is required in order to adequately address the issue.

In this paper, a number of 1540 activity portraying field LC waveforms are investigated to provide a detailed image of the waveforms' shapes, to show the limitations of conventional techniques, such as peak value monitoring, and propose and evaluate different techniques and criteria that can be employed to classify field waveforms based on their shape. Simple classification criteria are employed, using wavelet analysis, to distinguish between basic types. Further investigation and classification is performed on waveforms portraying discharges. Twenty different features, ten from time domain and ten from frequency domain are used. Two feature selection algorithms (student t-test and Minimum Redundancy–Maximum Relevance – or mRMR) and three classification algorithms (k-nearest neighbors, Naïve Bayes, Support Vector Machines) are employed. This paper complements previous work [23-29], providing a detailed image of field LC waveforms and proposing techniques capable to maximize the efficiency of the LC monitoring technique.

2 EXPERIMENTAL SET UP

The LC waveforms investigated in this paper have been recorded during a period exceeding six years, in two 150 kV Substations of the Transmission System of Crete, in Greece. The 150 kV Transmission network of Crete is exposed to intense marine pollution and the Greek Public Power Corporation (P.P.C. S.A.) has issued a large research project in collaboration with the University of Patras and the Technological Educational Institute of Crete, to monitor the behavior of insulators. Details about the sites, the monitoring system and the research project can be found in [23-29]. Waveforms investigated in this paper have been recorded on eighteen 150 kV post insulators (porcelain, RTV SIR coated and composite). The monitoring system employed incorporated the time-window technique to record waveforms [26-27]. Using this technique, a waveform of 480 ms around the largest peak value in each time window (e.g. a day) is recorded. The sampling rate is 2 kHz (960 data points per waveform). The techniques described in [26-28] have been applied in a group of more than 80,000 waveforms in order to remove waveforms portraying field noise, resulting to the 1540 waveforms which are investigated in this paper.

3 INVESTIGATION AND CLASSIFICATION

A schematic representation of the basic waveform shapes towards flashover is shown in Figure 1, with field waveforms selected and placed considering the waveform shapes and correlated stages of activity described in the literature [7, 9-14, 20-22]. The three discrete steps of Figure 1 correspond to the three basic stages of activity. The fact that field activity is not straight forward is shown with the use of two arrays showing at opposite directions. The dotted line at the lower right side indicates that within the investigated set of measurements a flashover has not been aloud, as the monitored insulators are live parts of the transmission system. Typical noise [26-28] is included with a typical noise waveform placed at the upper left side. It should be noted that since waveforms have been intermittently recorded on various insulators, Figure 1 is only hypothetical aiming to show that the basic waveform shapes reported in the literature in case of laboratory measurements, are also recorded in the field and also to depict a coherent hypothetical image of field LC waveforms' shape towards flashover based on relative literature regarding laboratory measurements.
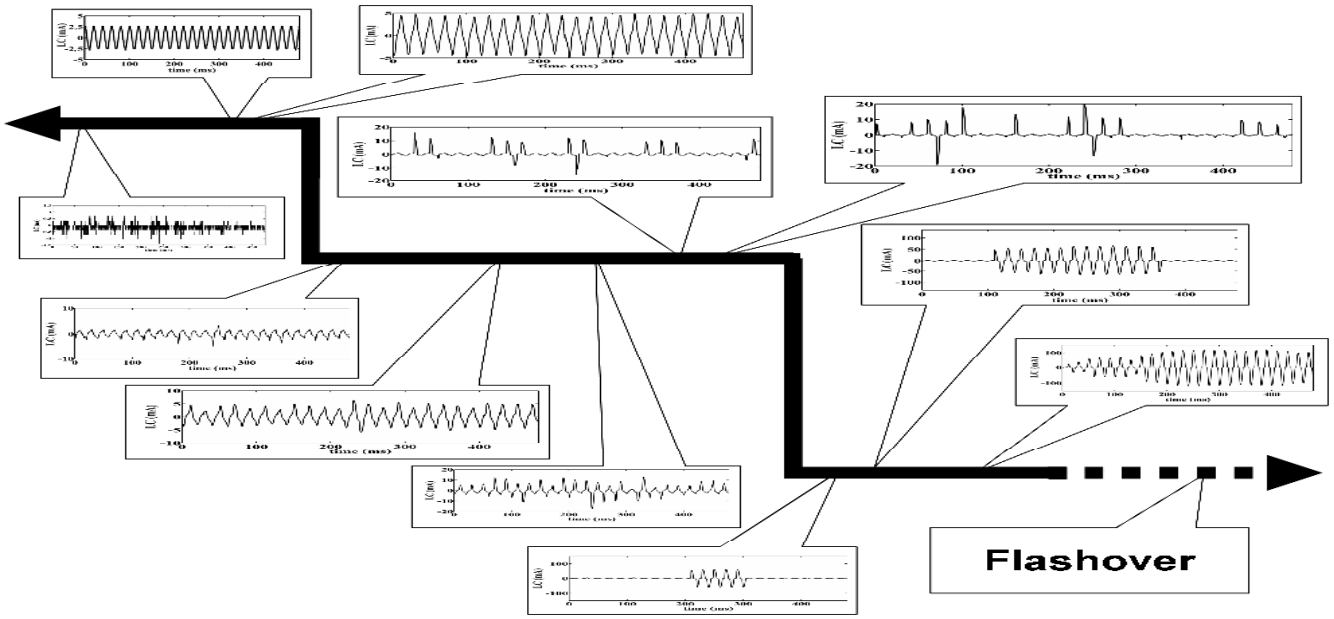
Figure 1. A hypothetical schematic representation of field waveforms as activity advances towards flashover.

However, the investigation of field waveforms revealed certain characteristics which call for further investigation, documented below.

3.1 SPIKES

The term "spikes" is used in this paper to describe single measurement points recorded far from the rest of the waveform and discriminate them from "pulses" which are consisted of more than one points. The presence of isolated spikes or Single Point Noise has been previously reported and investigated [26-28]. The Maximum and Minimum Point Smoothing technique [26-28] has been applied to the waveforms considered in this paper and isolated spikes have been removed. However, as shown in Figure 2, several waveforms have been recorded portraying a significant number of spikes. Further, the recorded spikes show a variety of amplitudes and they do not always follow the current's trend. It should be noted that in some cases spikes are localized in time, meaning that they appear only for a small number of periods as shown in Figure 2. It should also be noted that such spikes are also recorded at the transition from typical noise to sinusoids and vice versa, as shown in Figure 3. Spikes do not portray significant amplitude in the investigated set (always portraying a peak value under 50 mA). It is not clear whether these spikes illustrate electrical activity or noise. However, their presence can lead to misleading results, e.g. if the peak value is considered, and therefore such waveforms should be identified. To classify these waveforms the S_R ratio introduced in [27] can be employed. The S_R ratio is given by:

$$S_R = \frac{D1}{D\max} = \frac{D1}{\max(D_i)}$$

where D_i denotes the i-th value of the STD_MRA VECTOR and D_{max} the maximum value. The construction of the STD_MRA VECTOR requires the decomposition of the waveform using wavelet analysis and the calculation of the standard deviation of the details in each level, as described in [27]. The frequency bands for the different decomposition levels are shown in Table 1 [23].

Table 1. Frequency bands for different MRA levels.

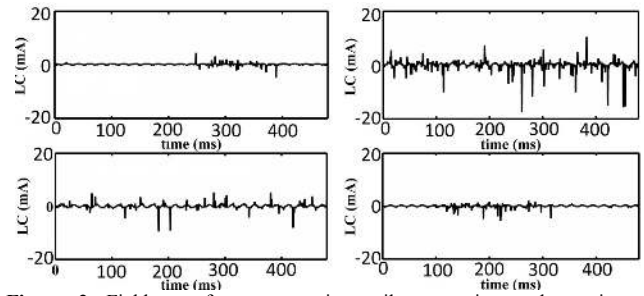| Decomposition Level	Approximation		Details	
1	0-500	(Hz)	500-1000	(Hz)
2	0-250	(Hz)	250-500	(Hz)
3	0-125	(Hz)	125-250	(Hz)
4	0-62.5	(Hz)	62.5-125	(Hz)
5	0-31.25	(Hz)	31.25-62.5	(Hz)
6	0-15.625	(Hz)	15.625-31.25	(Hz)

Figure 2. Field waveforms portraying spikes superimposed on sinusoid waveforms
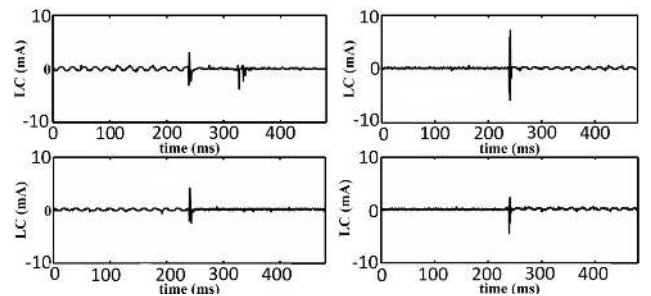

Figure 3. Spikes recorded at the transition from sinusoids to typical noise and vice versa.

The value of S_R can be used as a measure of the impact of spikes on the LC waveform. Waveforms similar to those depicted in Figures 2 and 3, having spikes as a dominant part, have an S_R value that equals to 1 and using this criterion a total of 220 waveforms is identified in the current set. As the S_R value decreases, spikes become less dominant. This means that the S_R ratio can be used to avoid misleading results due to the presence of spikes, (e.g. in the case of peak value monitoring), and also as a criterion for identifying waveforms having a specific impact of superimposed spikes as shown in Figure 4. The 20 waveforms in the investigated set having the highest S_R values, under 100%, are shown in Figure 5. However, as shown in Figure 5, as lower S_R limits are set some activity portraying waveforms may exceed the limit due to the presence of spikes. It should be noted however that in any case, waveforms with S_R lower than 50% are clear of spikes and that only 69 out of the 1540 waveforms have an S_R value between 100% and 50%.
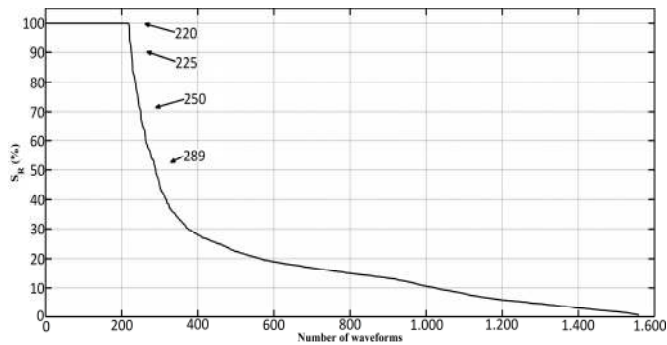

Figure 4. S_R ratio value Vs. the number of waveforms

3.2 SINUSOIDS

Sinusoids and distorted sinusoids usually recorded in the laboratory portray low peak values [7, 9-14]. However, in the considered set sinusoids of various peak values are included, with the largest recorded sinusoid having a peak value of almost 50 mA, as shown in Figure 6. Classifying sinusoids is a rather simple task since the presence of discharges has been well correlated with the odd harmonic content and especially the ratio of third to first harmonic [7, 10, 12-13, 30-33]. Therefore, the ratio D3/D5 of the STD_MRA VECTOR [23, 27], the frequency bands of which contains the third and first harmonic is used in this paper to identify sinusoid waveforms, with the value of 12% successfully identifying 367 sinusoid waveforms in the considered set. The peak value distribution of the 367 sinusoid waveforms is shown in Table II, showing that sinusoid waveforms may provide misleading results if the peak value and/or the charge is considered.

Table 2. Sinusoids.

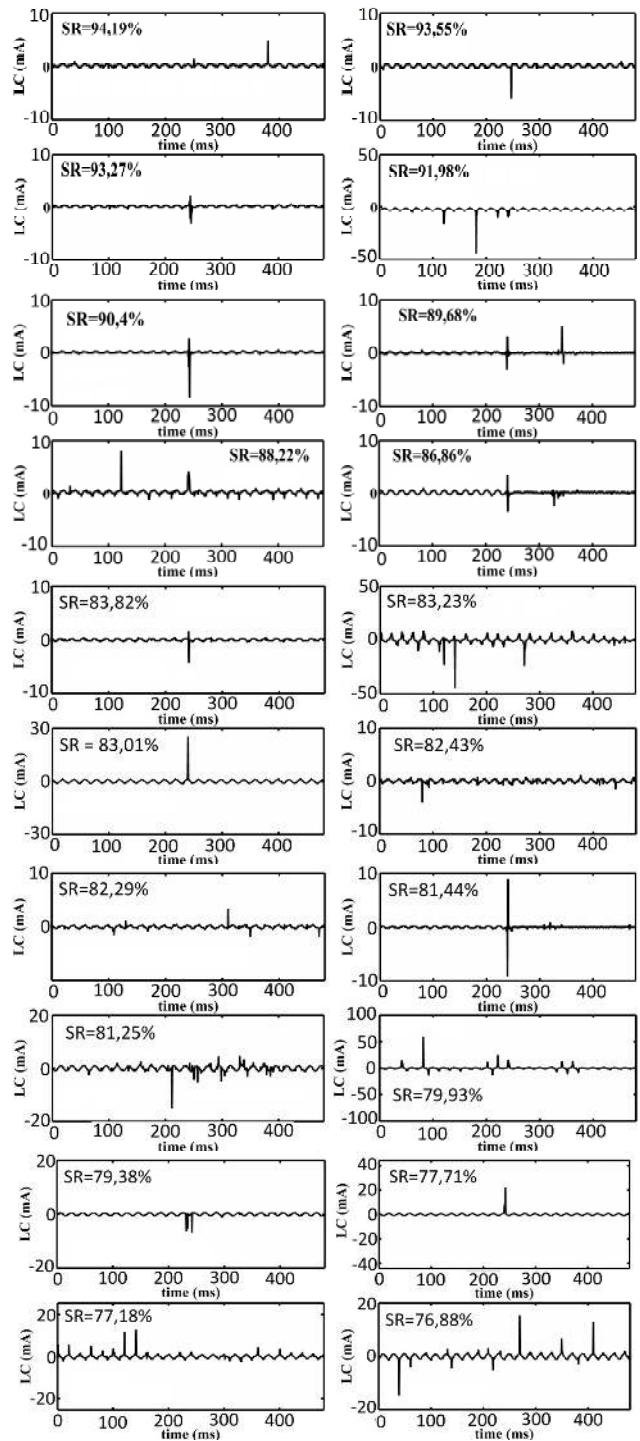| Peak value range (mA)	Number of waveforms
2.5-5	200
5-10	111
10-15	33
15-20	9
20-25	8
25-30	5
30-45	0
45-50	1

Figure 5. The 20 waveforms having the largest S_R value under 100%.
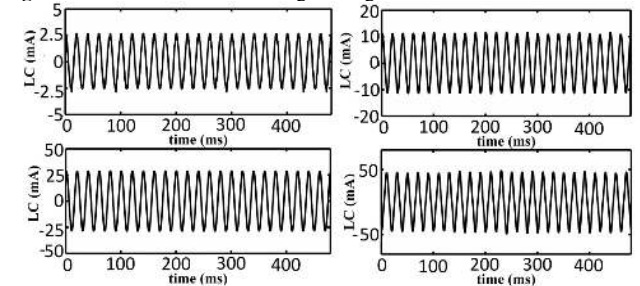

Figure 6. Sinusoids of various peak values recorded in the field.

Another issue concerning field sinusoid waveforms is sudden and gradual amplitude and distortion type changes as shown in Figure 7, which should be attributed to changes in the chemical content of the pollution layer. This issue should be considered especially if differential current values are calculated in order to detect arcing [34], since in such a case a sudden change may be taken for an arc. Such waveforms are also identified using the above mentioned criterion of the 12% value for the D3/D5 ratio.
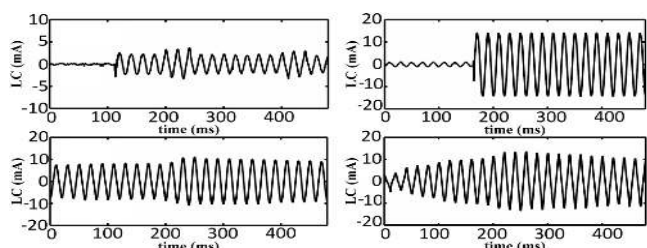

Figure 7. Sinusoids with amplitude and distortion type changes.

3.3 DISCHARGES

3.3.1 INVESTIGATION

The complexity of discharge portraying waveforms yields for the setting of added criteria in order to further categorize waveforms [24, 25]. It has been proposed [22] that the duration of discharges should be used to further categorize waveforms. An arbitrary duration of five half-cycles is set in this paper in order to classify waveforms in two different categories. A number of 387 discharge portraying waveforms are examined and classified by hand to the following two classes: C1 if the largest discharge portrayed in the waveform lasts four half-cycles or less, and C2 if the largest discharge portrayed in the waveform lasts five or more half-cycles. The distribution of the peak values for the two classes is shown in Table III. It should be noted that only waveforms of the second class exhibit peak values over 50 mA. Since both sinusoids and spikes are also recorded only under 50 mA, it can be concluded that the peak value can be representative of surface activity of large amplitude (over 50mA in this case), providing that waveforms portraying field noise [26-28] has been removed.

Table 3. Discharges.

Peak value range (mA)	Class 1 (C1): Number of waveforms	Class 2 (C2): Number of waveforms
2.5-5	63	14
5-10	65	63
10-15	27	37
15-20	7	26
20-25	2	17
25-30	3	13
30-35	1	8
35-40	0	6
40-50	2	8
50-60	0	3
60-70	0	6
70-80	0	3
80-90	0	2
90-100	0	2
100-140	0	5
>140	0	4

3.3.2 FEATURES

To automate the classification of discharge portraying waveforms to the classes C1 and C2, a set of 20 features is employed, as shown in Table 4. Features have been selected so as for the time and the frequency domain to be evenly represented and also considering the literature [6].

Table 4. Employed features.

No.	Feature (Time Domain - TD)	No.	Feature (Frequency Domain - FD)
1	Amplitude	11	Third to First Harmonic ratio: K3/K1
2	Mean	12	Fifth to First Harmonic ratio: K5/K1
3	Median	13	Fifth to Third Harmonic ratio: K5/K3
4	Variance	14	Total Harmonic Distortion ratio: THD
5	Standard deviation	15	Harmonic Distortion ratio: HD
6	Median absolute deviation	16	STD_MRA VECTOR ratio: D1/D5
7	Skewness	17	STD_MRA VECTOR ratio: D2/D5
8	Kurtosis	18	STD_MRA VECTOR ratio: D3/D5
9	Interquartile range	19	STD_MRA VECTOR ratio:D4/D5
10	Charge	20	Distortion Ratio: D_R

3.3.3 FEATURE SELECTION ALGORITHMS

Two different filter techniques are applied for feature selection. Filter techniques are generally divided into univariate and multivariate ones. The main advantages of such techniques are their simplicity, their low computational complexity and their independence from the classification algorithm. One univariate, the student's t-test [35-36] and one multivariate technique, the mRMR [37], are employed for feature selection. The main principle in both techniques is the calculation of a feature relevance score and the removal of low-scoring features.

T-test [35-36] is one of the simplest, oldest and most famous feature selection algorithms. The basic idea is to calculate t_i and the degrees of freedom and check whether the significance of the t_i value is high enough for each feature according to a standard table. The t_i value and the degrees of freedom are given by various equations depending on the form of the data. The form regarding unequal sample sizes and unequal variance is used in this paper.

The minimum Redundancy - Maximum Relevance (mRMR) algorithm [37] is a recently developed feature selection algorithm. Being a multivariate method, mRMR is capable of taking advantage of the complex dependencies between features. Its goal is to select a feature subset that bares the minimum redundancy between the selected features and the maximum relevance to the classes. Several values can be employed to calculate redundancy and relevance, with the mutual information being used in this paper.

3.3.4 CLASSIFICATION ALGORITHMS

Three of the most commonly used classification techniques [38] are employed: the k-nearest neighbors' classifier (knn) [38-39], the Naïve Bayesian classifier [38, 40-41] and Support Vector Machines (SVMs) [38, 42-43].

The k-nearest neighbors' classifier [38-39] is a simple, easy to implement classifier that assigns an object to a class based

on the classes of its k nearest neighbors. Several distances can be used to find the nearest neighbors, with the Euclidian distance being used in this paper.

The Naïve Bayes classifier [38, 40-41] is a well known simple probabilistic classifier based on Bayes theory. It is one of the oldest classification algorithms and despite its simplicity, it is known to be rather effective. The algorithm assumes that features are independent and its efficiency is largely dependent on feature selection and also on the data used for training.

Support Vector Machines (SVMs) [38, 42-43] are considered as one of the most accurate machine learning classifiers. The SVM algorithm is a supervised learning method that addresses the problem of linear and non linear classification by finding the maximum margin hyperplane that best separates the classes. Non-linear SVMs map the training samples from the input space into a higher-dimensional feature space with the use of some mapping function, also known as kernel function. Several kernel functions can be used and the Radial Base Function has been employed in this paper. The mapping procedure resembles the hidden neuron layer of neural networks. However, SVMs do not suffer from local minima or overfitting, as neural networks do, they have the advantage of automatically selecting their model size and provide superior generalization ability by maximizing the margin of separation.

3.3.5 RESULTS

Twenty runs were conducted for each feature set and classification algorithm. In case of knn, in each run, 40% of the data was used as the training set, 10% as the evaluation set (testing different values for k, from 3 to 15) and 50% as the test set. In case of the Naïve Bayes classifier, in each run, 50% of the data were used as the training set and 50% as the test set. In case of SVMs, in each run, 40% of the data was used as the training set, 10% as the evaluation set (selecting optimal values for c and gamma parameters using grid search) and 50% as the test set. The mean identification success rate (percentage) for the 20 runs is calculated and overall results are shown in Table 5.

Table 5. Results for different feature sets and classification algorithms.

Features	TD {1-10}	FD {11-20}	All {1-20}	t-test {1, 3-11, 13-17, 19-20}	mRMR {3, 5, 7, 8, 11, 13, 15, 16, 18, 19}
knn	82.13%	86.77%	85.22%	83.85%	85.74%
Naïve Bayes	69.41%	77.66%	73.02%	73.88%	86.43%
SVMs	82.48%	88.49%	87.80%	87.80%	90.21%

Several results portrayed in Table 5 should be noted. At first it is shown that frequency domain features give better results for all three classification algorithms compared to the time domain features or the time domain features along with the frequency domain features. This fact, on the one hand shows that adding more features does not necessarily mean higher

identification rate and on the other hand shows the higher correlation between the frequency domain and the waveform shape.

Regarding feature selection, it is shown that the student t-test is ineffective since it removes only 3 features. It should also be noted that the t-test features gives worst results compared to the frequency domain set and better results compared to the time domain set in all cases. The mRMR algorithm removes 10 features and keeps 4 features from the time domain and 6 features from the frequency domain. It should be noted that, regarding time domain features, the algorithm removes, among others, the commonly used values of amplitude and charge and keeps only the median, the standard deviation, skewness and kurtosis. Regarding frequency domain features, the algorithm keeps the third to first harmonic ratio, the fifth to third harmonic ratio and the Harmonic Distortion but not the fifth to first harmonic ratio and the Total Harmonic Distortion ratio. The algorithm also keeps all ratios of the STD_MRA VECTOR values except for D2/D5.

Regarding the classification, the superiority of SVMs is documented in every case. The significance of feature selection for the Naïve Bayes classifier is underlined. It is shown that the mRMR feature set produces the best results for all three algorithms with the only exception of the knn algorithm that shows slightly better results for the frequency domain set. It is noteworthy that knn and SVMs have similar results in case of the time domain features (difference of 0.35%) and that overall best results are recorded in case of the SVMs using the mRMR feature set. These results underline two discrete approaches related to complexity and calculation cost: the first approach is a simple identification using only time domain values and the knn algorithm (success percentage over 82%) and the second is a more complicated approach employing SVMs and time and frequency domain features selected using mRMR (success percentage over 90%).

4   CONCLUSION

It is widely accepted that field measurements are required in order to acquire an exact image of surface activity and insulators' performance. However, field LC waveforms have not been thoroughly investigated and researchers commonly record and monitor extracted values such as the peak value and the charge from the LC waveform. These values, however, are not always representative of the waveforms' shape and can be misleading. In this paper, a large number of field LC waveforms are investigated and classification techniques are employed in order to investigate the issue and offer tools to maximize the efficiency of field LC monitoring. Wavelet analysis and the STD_MRA technique is employed to perform basic identification. Further, three classification algorithms (knn, Naïve Bayes, SVMs) and two feature selection algorithms are employed in order to automate the classification of discharge portraying waveforms. 20 different features are employed, 10 from the time domain and 10 from the frequency domain. A total of 5 feature sets are employed in combination with the classification algorithms.

The main conclusions are as follows.

1) Field LC waveforms confirm the basic shapes reported in the literature referring to laboratory measurements. However, some peculiarities regarding field LC waveforms are recorded, such as the occurrence of spikes, sinusoids of exceptionally large amplitude and sinusoids portraying gradual and sudden amplitude and distortion type changes. Such waveforms show that classification between basic waveform types is required in order to avoid misleading results.

2) Wavelet STD_MRA analysis can be used to identify basic waveform types. The S_R ratio previously employed for investigating waveforms of low amplitude, can also be employed to identify waveforms portraying spikes. Another ratio of the values from the STD_MRA VECTOR (D3/D5 in this paper) can be used to identify sinusoid waveforms. Waveforms portraying discharges can be indirectly identified using the above ratios.

3) Discharge portraying waveforms are further categorized in two classes in relation to the duration of portrayed discharges. It is shown that waveforms of both classes may exhibit small and medium peak values (up to 50mA), but only waveforms of the second class (discharges with duration over 5 half-cycles) exhibit significantly large peak values (over 50mA)

4) The previous conclusion combined with the peak values distribution for spikes and sinusoids yield the result that the LC peak value can be a trustworthy indication of activity and waveform type only in case of significant activity that corresponds to significant peak value levels (in this case, over 50mA).

5) Features from the frequency domain provide better results compared to features from the time domain and also to a set containing both. This shows the correlation of the waveforms' shape with the frequency content and hints that using more features may lead to worst results.

6) Feature selection algorithms can be used to enhance the classification performance and reduce the number of features used.

7) Results show the superior performance of SVMs and of the feature set provided by the mRMR algorithm.

8) If one is to consider the calculation complexity, results underline two different approaches: the first being to employ the time domain features and the knn algorithm (success percentage over 82%) and the second one being to employ SVMs and features from both time and frequency domain, selected using the mRMR algorithm (success percentage over 90%)

The work described in this paper complements previous work coping with field related noise and the data accumulation problem, providing a full image of field LC waveforms and identification approaches that may be used to significantly enhance the effectiveness of field LC monitoring.

REFERENCES

[1] CIGRE WG 33-04, "The measurement of site pollution severity and its application to insulator dimensioning for A.C. systems", Eletra, No. 64, pp. 101-115, 1979.

[2] CIGRE WG 33-04, TF 01, Polluted insulators: a review of current knowledge, Cigre Publications, 1998.

[3] IEC/TS 60815, Selection and dimensioning of high-voltage insulators intended for use in polluted conditions, IEC, 2008.

[4] S. Gubanski, "Ageing of composite insulators", in *Ageing of Composites*, Woodhead Publishing in Materials, United Kingdom, 2008.

[5] CIGRE WG B2.03, "Guide for the establishment of naturally polluted insulator testing stations", Cigre Publications, 2007.

[6] D. Pylarinos, K. Siderakis and E. Pyrgioti "Measuring and analyzing leakage current for outdoor insulators and specimens", Rev. Advanced Materials Sci., Vol. 29, No. 1, pp. 31-53, 2011.

[7] M. A. R. M. Fernando and S. M. Gubanski, "Leakage current patterns on contaminated polymeric surfaces", IEEE Trans. Dielectr. Electr. Insul., Vol. 6, No. 5, pp. 688–694, 1999.

[8] I. J. S. Lopes, S. H. Jayaram and E. A. Cherney, "A Method For Detecting The Transition from Corona from Water Droplets to Dry-Band Arcing on Silicone Rubber Insulators", IEEE Trans. Dielectr. Electr. Insul., Vol. 9, No. 6, pp. 964–971, 2002.

[9] I. A. Metwally, A. Al-Maqrashi, S. Al-Sumry and S. Al-Harthy, "Performance Improvement of 33kV line-post insulators in harsh environment", Electr. Power Syst. Res., Vol. 76, No. 9-10, pp. 778-785, 2006.

[10] A. H. El-Hag, S. H. Jayaram and E. A. Cherney, "Fundamental and low frequency harmonic components of leakage current as a diagnostic tool to study aging of RTV and HTV silicone rubber in salt-fog", IEEE Trans. Dielectr. Electr. Insul., Vol. 10, No. 1, pp. 128–136, 2003.

[11] J. Li, W. Sima, C. Sun and S. A. Sebo, "Use of Leakage Current of Insulators to Determine the Stage Characteristics of the Flashover Process and contamination Level Predicition", IEEE Trans. Dielectr. Electr. Insul., Vol. 17, No. 1, pp. 128–136, 2010.

[12] T. Suda, "Frequency characteristics of leakage current waveforms of an artificially polluted suspension insulator", IEEE Trans. Dielectr. Electr. Insul., Vol. 8, No. 4, pp. 705–709, 2001.

[13] T. Suda, "Frequency Characteristics of Leakage Current Waveforms of a String of Suspension Insulators", IEEE Trans. Power Deliv., Vol. 20, No. 1, pp. 481–487, 2005.

[14] S. Chandrasekar, C. Kalaivanan, A. Cavallini and G. C. Montanari, "Investigations on Leakage Current and Phase Angle Characteristics of Porcelain and Polymeric Insulator under Contaminated Conditions", IEEE Trans. Dielectr. Electr. Insul., Vol. 16, No. 2, pp. 574-583, 2009.

[15] H. H. Kordkheili, H. Abravesh, N. Tabasi, M. Dakhem and M. M. Abravesh, "Determining the Probability of Flashover Occurrence in Composite Insulators by Using Leakage Current Harmonic Components", IEEE Trans. Dielectr. Electr. Insul., Vol. 17, No. 2, pp. 502-512, 2010.

[16] Waluyo, P. M. Pakpahan, Suwarno and M. A. Djauhari, "Study on Leakage Current Waveforms of Porcelain insulator due to various Artificial Pollutants", World Academy of Sci., Eng. Techn., Vol. 32, pp. 293–298, 2007.

[17] I. Garniwa, B. Sudiarto and R. S. Ansorulah, "Effect of pollutant type and concentration on harmonic characteristic of leakage current on resin epoxy insulator", 2nd Indonesia Japan Joint Scientific Sympos., pp. 1-6, 2006.

[18] F. Aulia, F. David, E. P. Waldy and H. Hazmi, "The leakage current analysis of 20 kV porcelain insulator contaminated by salt moisture and cement dust in Padang area", IEEE 8th Int'l. Conf. Properties and Applications of Dielectr. Materials, Bali, Indonesia, pp. 384-387, 2006

[19] N.A.B.T. Mahyudin, *Study on Leakage Current of Insulators due to Environmental Pollutans*", Bachelor Thesis, Faculty of Electrical Engineering, Universiti Teknologi Malaysia, 2011.

[20] C. S. Richards, C. L. Benner, K. L. Butler-Purry and B. D. Russell, "Electrical Behavior of Contaminated Distribution Insulators Exposed to Natural Wetting", IEEE Trans. Power Deliv., Vol. 18, No. 2, pp. 551-558, 2003.

[21] K. Siderakis, D. Agoris and S. Gubanski, "Influence of heat conductivity on the performance of RTV SIR coatings with different fillers", J. Phys. D: Appl. Phys., Vol. 38, No. 19, pp. 3682-3689, 2005.

[22] M. Sato, A. Nakajima, T. Komukai and T. Oyamada, "Spectral Analysis of Leakage Current on Contaminated Insulators by Auto Regressive Method", IEEE Conf. Electr. Insul. Dielectr. Phenomena (CEIDP), pp. 64–66, 1998.

[23] D. Pylarinos, K. Siderakis, E. Pyrgioti, E. Thalassinakis and I. Vitellas, "Automating the classification of field leakage current waveforms", Eng. Technol. Appl. Sci. Res., Vol. 1, No. 1, pp. 8-12, 2011.

[24] D. Pylarinos, K. Siderakis, E. Pyrgioti, I. Vitellas and E. Thalassinakis, "Monitoring leakage current waveforms in the field", DEMSEE 5th Int'l. Conf. Technical Exhibit on Deregulated Electricity Market issues in South-Eastern Europe, Sitia, Greece, 2010.

[25] D. Pylarinos, K. Siderakis, E. Thalassinakis, E. Pyrgioti and I. Vitellas, "Investigation of leakage current waveforms recorded in a coastal high voltage substation", Eng. Technol. Appl. Sci. Res., Vol. 1, No. 3, pp. 63-69, 2011.

[26] D. Pylarinos, K. Siderakis, E. Thalassinakis, E. Pyrgioti, I. Vitellas and S. L. David, "Online applicable techniques to evaluate field leakage current waveforms", Electr. Power Syst. Res., Vol. 84, No. 1, pp. 65-71, 2012.

[27] D. Pylarinos, K. Siderakis, E. Pyrgioti, E. Thalassinakis and I. Vitellas, "Impact of noise related waveforms on long term field leakage current measurements", IEEE Trans. Dielectr. Electr. Insul., Vol. 18, No. 1, pp. 122-129, 2011.

[28] D. Pylarinos, K. Siderakis, E. Pyrgioti , E. Thalassinakis and I. Vitellas, "Investigating and overcoming the noise and data size problems in long term field leakage current monitoring", 17th Int'l. Sympos. High Voltage Eng. (ISH), Hannover, Germany, paper no. F032, 2011.

[29] D. Pylarinos, K. Siderakis, E. Thalassinakis, I. Vitellas and E. Pyrgioti, "Recording and managing field leakage current waveforms in Crete. Installation, measurement, software development and signal processing", ISAP 16th Int'l. Conf. Intelligent System Applications to Power Systems, Hersonissos, Crete, Greece, pp. 1-6, 2011.

[30] J.H. Kim, W.C. Song, J. H. Lee, Y.K. Park, H.G. Cho, Y.S. Yoo and K.J. Yang, "Leakage Current Monitoring and Outdoor Degradation of Silicone Rubber", IEEE Trans. Dielectr. Electr. Insul., Vol. 8, No. 6, pp. 1108-1115, 2001.

[31] Y. Zhu, S. Yamashita, N. Anami and M. Otsubo, "Leakage Current Analysis and Electric Field Calculation in Salt Fog Ageing Test on Polymer Insulation Material", IEEE Conf. Electr. Insul. Dielectr. Phenomena (CEIDP), pp. 92-95, 2003.

[32] A. H. El-Hag, A. N. Jahromi and M. Sanaye-Pasand, "Prediction of Leakage Current of Non-ceramic Insulators in Early Aging Period", Electr. Power Syst. Res., Vol. 78, No. 10, pp. 1686-1692, 2008.

[33] K. Siderakis and D. Agoris, "Performance RTV Silicone Rubber Coatings Installed in Coastal Systems", Electr. Power Syst. Res., Vol. 78, No. 2, pp. 248-254, 2008.

[34] M. Otsubo, T. Hashiguchi, C. Honda, O. Takenouchi, T. Sakoda and Y. Hashimoto, "Evaluation of insulation performance of polymeric surface using a novel separation technique of leakage current", IEEE Trans. Dielectr. Electrical Insulat, Vol. 10, No. 6, pp. 1053-1060, 2003.

[35] R.A. Johnson and G.K. Bhattacharyya, *Statistics: Principles and Methods*, John Wiley & Sons Inc, 6th Edition, 2010.

[36] S. Welleck, *Testing Statistical Hypothesis of Equivalence*, Chapman and Hall, CRC, Boca Raton, Florida, USA, 2003.

[37] H. Peng, F. Long and C. Ding, "Feature selection based on mutual information: criteria of max-dependency, max-relevance, and min-redundancy", IEEE Trans. Pattern Anal. Mach. Intell., Vol. 27, No. 8, pp. 1226-1238, 2005.

[38] X. Wu, V. Kumar, J. R. Quinlan, J. Ghosh, Q. Yang, H. Motoda, G. J. McLachlan, Angus Ng, B. Liu, P. S. Yu, Z. H. Zhou, M. Steinbach, D. J. Hand and D. Steinberg, "Top 10 algorithms in data mining", Knowledge and Information Systems, Vol. 14, No. 1, pp. 1–37, 2008.

[39] T. M. Cover and P. E. Hart, "Nearest neighbor pattern classification", IEEE Trans. Inf. Theory, Vol. 13, No. 1, pp. 21–27, 1967.

[40] C. M. Bishop, *Pattern Recognition and Machine Learning*, Springer, 2006.

[41] V. N. Vapnik, *The Nature of Statistical Learning Theory*, Springer, USA, 2000.

[42] C. J. C. Burges, "A Tutorial on Support Vector Machines for Pattern Recognition", Data Min. Knowl. Disc., Vol. 2, No. 2, pp. 121–167, 1998

[43] J. A. K. Suykens, "Support vector machines: A nonlinear modelling and control perspective", Eur. J. Control, special issue on fundamental issues in control, Vol. 7, pp. 311-327, 2001

Dionisios Pylarinos was born in Athens, Greece in 1981. He received a Diploma degree in Electrical and Computer Engineering in 2007 and the Ph.D. degree in the same field in 2012 from the University of Patras, Greece. He is presently a scientific consultant for the Public Power Corporation (PPC), Greece. He is a member of the Technical Chamber of Greece. His research interests include outdoor insulation, electrical discharges, leakage current, signal processing and pattern recognition.

Konstantinos Theofilatos was born in Patras in 1983. He graduated in 2006 from the Department of Computer Engineering and Informatics of the University of Patras, Greece. In 2009, he received a Master's degree from the same department. Since 2009, he has been a Ph.D. degree candidate in the same department. He is a member of the Pattern Recognition Laboratory (prlab.ceid.upatras.gr) since 2006. His research interests include computational intelligence, machine learning, data mining, bioinformatics, web technologies and time series forecasting and signal processing.

Kiriakos Siderakis was born in Iraklion in 1976. He received a Diploma degree in Electrical and Computer Engineering in 2000 and the Ph.D. degree in 2006 from the University of Patras. Presently, he is a Lecturer at the Department of Electrical Engineering, at the Technological Educational Institute of Crete. His research interests include outdoor insulation, electrical discharges, high voltage measurements and high voltage equipment diagnostics and reliability. He is a member of the Greek CIGRE and of the Technical Chamber of Greece.

Emmanuel Thalassinakis received the Diploma in Electrical and Mechanical Engineering and also the Ph.D. degree from the National Technical University of Athens. After working for the Ministry of the Environment, in 1991 he joined the Public Power Corporation (PPC) where he is now Assistant Director of the Islands Network Operations Department.

Isidoros Vitellas was born in 1954 in Greece. He has a Diploma in Electrical Engineering and the Ph.D. degree in the same field. He is currently Director of the Islands Network Operations Department in PPC (Public Power Corporation) Athens, Greece.

Antonio T. Alexandridis (M'88) received a Diploma in electrical engineering from the Department of Electrical Engineering of the University of Patras, Greece, in 1981. In 1987, he received the Ph.D. degree from the Electrical and Computer Engineering Department of the W. Virginia University, USA. He is a Professor and Head of the Power Systems Division the Department of Electrical and Computer Engineering of the University of Patras. His research interests include control theory, nonlinear dynamics, optimal control, eigenstructure assignment, passivity and advanced control applications on power systems and drive systems. His current interests are focused on Renewable Power Generation Control and Stability (wind generators, PV systems etc.). He is a member of the Technical Chamber of Greece.

Eleftheria Pyrgioti was born in 1958 in Greece. She received the Diploma degree in electrical engineering from Patras University in 1981 and the Ph.D. degree from the same University in 1991. She is an assistant professor at the department of Electrical and Computer Engineering at the University of Patras. Her research activity is directed to the high voltage, lightning protection, insulation coordination, distributed generation. She participates in the permanent committee TE 63 of ELOT (Hellenic Organization for Standardization) since 1989 and is a member of the Greek CIGRE and the Technical Chamber of Greece.